

Voltage-Controlled Spin Selection in a Magnetic Resonant Tunnelling Diode.

A. Slobodskyy, C. Gould, T. Slobodskyy, C.R. Becker, G. Schmidt, and L.W. Molenkamp
Physikalisches Institut (EP3), Universität Würzburg, Am Hubland, D-97074 Würzburg, Germany
 (Dated: March 7, 2003.)

We have fabricated all II-VI semiconductor resonant tunneling diodes based on the (Zn,Mn,Be)Se material system, containing dilute magnetic material in the quantum well, and studied their current-voltage characteristics. When subjected to an external magnetic field the resulting spin splitting of the levels in the quantum well leads to a splitting of the transmission resonance into two separate peaks. This is interpreted as evidence of tunneling transport through spin polarized levels, and could be the first step towards a voltage controlled spin filter.

PACS numbers: 72.25.Dc, 85.75.Mm

The physics governing spin injection and detection in semiconductor structures is now well understood [1, 2, 3]. The problems associated with the impedance mismatch between a magnetic layer and the semiconductor can be overcome, e.g. by using dilute magnetic semiconductor injectors [4, 5, 6], or by fitting metallic magnetic contacts with tunnel barriers [7]. However, these options can only be utilised to transfer majority spin from the magnetic material into the non-magnetic layer and, similar to the situation in magnetic metallic multilayers, contacts with different shape anisotropy must be used when the direction of the spin of the electrons in the semiconductor is to be detected. Rather than having to use an external magnetic field to switch the contact magnetisation, it would be very desirable to have devices where the spin character of the injected or detected electrons could be voltage selected. Here we report on the successful operation of a magnetic resonant tunnelling diode (RTD), which we hope will prove useful for voltage controlled spin polarised injection and detection [8].

The idea behind the RTD scheme is fairly straightforward but its realisation was previously hampered by material issues [9]. Since the well is made of magnetic material, the energy levels in the well will split into spin-up and spin-down states, as sketched in Fig. 1(b). By selectively bringing the spin-up or spin-down state into resonance, one can dramatically increase the transmission probability of the desired spin species.

In this paper, we describe our experimental investigations of an all II-VI semiconductor RTD based on ZnBeSe, and with a ZnMnSe dilute magnetic semiconductor (DMS) quantum well. In the presence of a (constant) magnetic field, the DMS exhibits a giant Zeeman splitting that, at low temperatures, leads to an energy splitting of the Zeeman levels in the conduction band of about 15 meV at fields of one to two Tesla. Our samples show typical RTD-like current-voltage (I-V) characteristics with peak to valley ratios of over 2.5 to one. As a function of applied magnetic field, the transmission resonance of the I-V curve splits into two peaks with a splitting corresponding to the separation of the energy levels in the well.

The investigated II-VI semiconductor heterostructures were grown by molecular-beam epitaxy on insulating

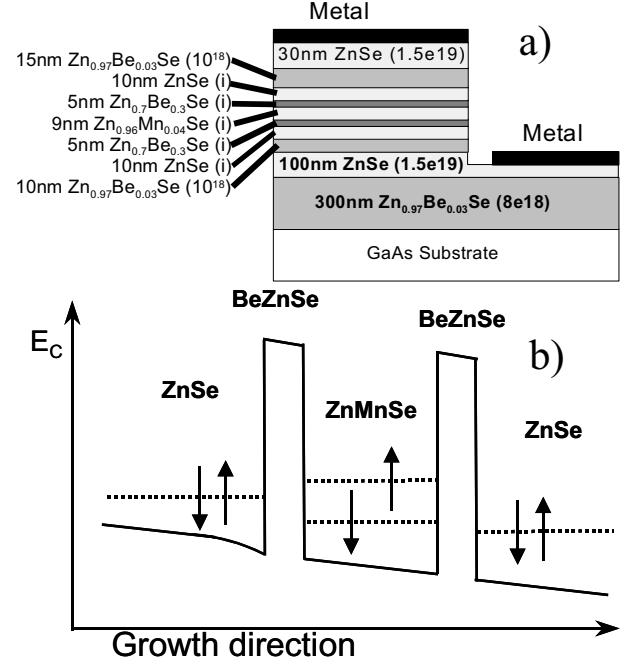


FIG. 1: a) Layer structure of the device and b) schematic view of resonance tunnel diode band structure under bias.

GaAs substrates. The active region of the device consists of a 9 nm thick undoped Zn_{0.96}Mn_{0.04}Se quantum well, sandwiched between two 5 nm thick undoped Zn_{0.7}Be_{0.3}Se barriers. The complete layer structure is shown in Fig. 1 along with a schematic of the potential energy profile of the double-barrier structure under bias. The bottom 300 nm of Zn_{0.97}Be_{0.03}Se, highly n-type doped with iodine to a concentration of $n=8 \times 10^{18} \text{ cm}^{-3}$, as well as the 15 and 10 nm thick Zn_{0.97}Be_{0.03}Se layers with $n=1 \times 10^{18} \text{ cm}^{-3}$ in the injector and collector contain 3% Be in order to be lattice matched to the GaAs substrate. The barrier layers are clearly not lattice matched to the substrate, but are sufficiently thin to be grown as fully strained epitaxial layers. The heterostructure was patterned into square mesas with side of 100, 120 and 150 μm by optical lithography with positive photoresist followed by metal evaporation and lift off.

Special care must be taken in order to obtain good

ohmic contacts to the II-VI semiconductor. For the top contact, this can be achieved by in-situ growth of a metal contact layer consisting of 10 nm Al to achieve good contact, 10 nm Ti as a diffusion barrier, and 30 nm Au to avoid oxidation. This procedure reliably yields contact resistivities of the order of $10^{-3}\Omega\cdot\text{cm}^2$. Since the bottom contact can only be fabricated after processing, it must rely on an ex-situ technique where the contact resistivity is typically 1-3 orders of magnitude higher. Its resistance is kept reasonably low by a combination of the incorporation of a highly n doped 100 nm ZnSe contact layer in the heterostructure, and the use of a relatively large ($500^2\mu\text{m}^2$) Ti-Au contact pad.

The samples were inserted into a ^4He bath cryostat equipped with a 6 Tesla superconducting magnet, and were investigated using standard low noise electrical characterization techniques. Precautions were taken to prevent problems associated with the measurement circuit going into oscillations. A stabilised voltage source was used to apply bias to the circuit, which consists of the RTD, a 33 Ohm reference resistance in series and a 40 Ohm resistor in parallel. Such a setup is known to prevent bi-stability of the circuit in the region of negative differential resistance [10]. By measuring the voltage drop over the RTD and the reference resistor as the bias voltage is swept, I-V curves of the RTD can be extracted. The absence of charging in the device was confirmed by comparing I-V curves with different sweep direction [11].

We studied devices with Mn concentrations of 4% and 8% in the quantum well layer. The layers thicknesses of the 4% sample are given in Fig. 1, whereas those for the 8% Mn sample are all 6% thinner. For structures with 4% Mn in the well, the first resonance for positive bias occurs at 105 mV and has a peak to valley ratio of 2.5 whereas for the 8% Mn sample the resonance is at 127 mV with a peak to valley ratio 2.25. The size of the mesas had no effect on the position and strength of the resonance.

I-V characteristics of the RTDs were measured in different magnetic fields in the range from 0 to 6T applied either perpendicularly to, or in the plane of the quantum well. The results for perpendicular magnetic fields are presented in Fig. 2 (lines). For clarity, subsequent curves are offset by $10\mu\text{A}$. It is clear from the figure that the resonance is split into two parts and that the splitting grows as a function of magnetic field. At 6 Tesla, the separation between the maxima of the split peaks is 36.5 mV and 42 mV for 4% and 8% Mn samples respectively. The broader feature which can be seen most prominently in the zero field curve at approximately 165 mV (180 mV) for the 4% (8%) of Mn samples is an LO phonon replica [10].

To explain the magnetic field-induced behaviour of the resonance, we develop a model based on the Giant Zeeman splitting for the spin-split levels in the DMS quantum well. First, we extract the series contact resistance of the RTD from the measured I-V curve at zero magnetic field [11, 12]. Then we assume that each of the two

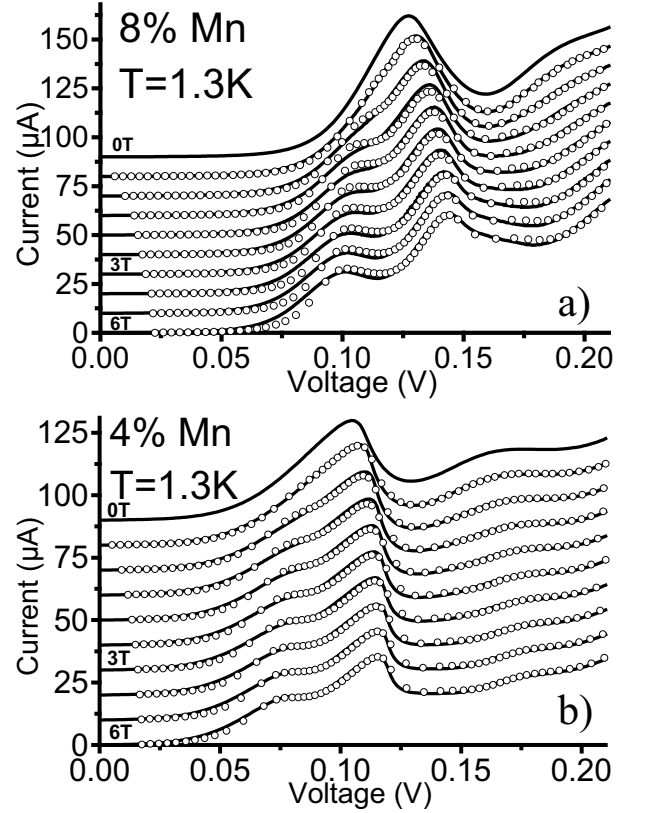


FIG. 2: Experimental (lines) and modeled (circles) I-V curves for a resonance tunnel diode with a) $\text{Zn}_{0.92}\text{Mn}_{0.08}\text{Se}$ and b) $\text{Zn}_{0.96}\text{Mn}_{0.04}\text{Se}$ in the quantum well. Curves taken in 0.5T intervals from 0 to 3T and in 1T intervals from 3T to 6T.

spin split levels have the same conductance, and that each therefore carries half of the current in the device.

We neglect the slight relative change of barrier height caused by the change in energy of the levels, and assume that the conductivity of each level is independent of magnetic field in the sense that for the same alignment between the emitter Fermi level and the well level, the conductivity will be the same. In other words, the conductivity of each level as a function of applied voltage in the presence of a magnetic field can be given by a simple translation of the zero field curve by a voltage corresponding to the energy shift of the pertinent spin level in the well.

After translation, we add the conductivity contributions of both the spin-up and the spin-down curves, and reinsert the series resistance to yield a modelled I-V curve at a given magnetic field. By comparing this I-V curve with the actual experimental curve at 6 Tesla, we determine an optimal value of 330 Ohm (900 Ohm) for the series resistance for the 8% (4%) Mn sample. Using this value of the series resistance for all modelled curves, and fitting the modelled curves at each field to the experimental ones, we extract the voltage splitting of the levels ΔV as a function of magnetic field. Fig. 2 shows the modelled I-V curves as the circles, which compare very

well with the experimental data presented as the solid lines in the figure.

We now compare the values of ΔV extracted from this fitting procedure to the expected behaviour of the spin levels in the wells. The spin level splitting ΔE of the DMS as a function of magnetic field B is given by a modified Brillouin function [13]:

$$\Delta E = N_0 \alpha x s_0 B_s (s g \mu_B B / k_B (T + T_{eff})),$$

where $N_0 \alpha$ is the s-d exchange integral, x , s , and g are the manganese concentration, manganese spin, and g-factor respectively, and μ_B is the Bohr magnetron. B_s is the Brillouin function of spin s . s_0 and T_{eff} are, respectively, the effective manganese spin and the effective temperature. These phenomenological parameters are needed to account for Mn interactions. Taking established values of $T_{eff} = 2.24$ K, $s_0 = 1.13$ [14] for $x = 8\%$ ($T_{eff} = 1.44$ K, $s_0 = 1.64$ for $x = 4\%$) and $N_0 \alpha = 0.26$ eV [15] from the literature, we obtain values for ΔE which are plotted as the solid lines in Fig. 3(a) for temperatures of 1.3, 4.2, and 8K and for Mn concentrations of 4% and 8%. These curves are compared with the values of ΔE extracted from experiment (symbols in the same figure) for measurements taken at the respective temperatures. It is important to note that in order to correctly fit the amplitude to the Brillouin function, the measured values of ΔV must be divided by a lever arm of 2.1. The agreement between the magnetic field dependence of the experimental values and the Brillouin function is remarkable, suggesting that our model of two spin level splitting in a magnetic field captures the essential character of the device. More over an identical value of the lever arm is found for both the 4% and 8% Mn samples.

The existence of a lever factor between the experimental voltage splitting and the theoretical energy splitting in the well is a well-known feature of RTDs. It occurs because only part of the voltage applied to the device is dropped over the first barrier, and thus effective in determining the alignment condition for the resonance. Furthermore, extracting the lever factor for our diode by comparing the observed voltage splitting in the $B=0$ I-V curve between the first resonance and the phonon replica to the known LO phonon energy of ZnSe (31.7 meV) [16] also yields a lever arm of around 2.

In Fig. 3(b) we compare measurements at 3T with magnetic field in the plane of, and perpendicular to the quantum well. The curves are offset for clarity. Evidently, the peaks in the I-V curve for in-plane magnetic field are broader than those for perpendicular field and are shifted slightly towards higher bias voltages. This effect is known from GaAs based RTDs [17] and can be explained in terms of momentum conservation. For magnetic field in plane (perpendicular to the motion of the electrons), the Lorentz force will give the electrons an in-plane momentum. The conservation of in-plane momentum during the tunnelling process forces electrons to tunnel into finite momentum states of the quantum

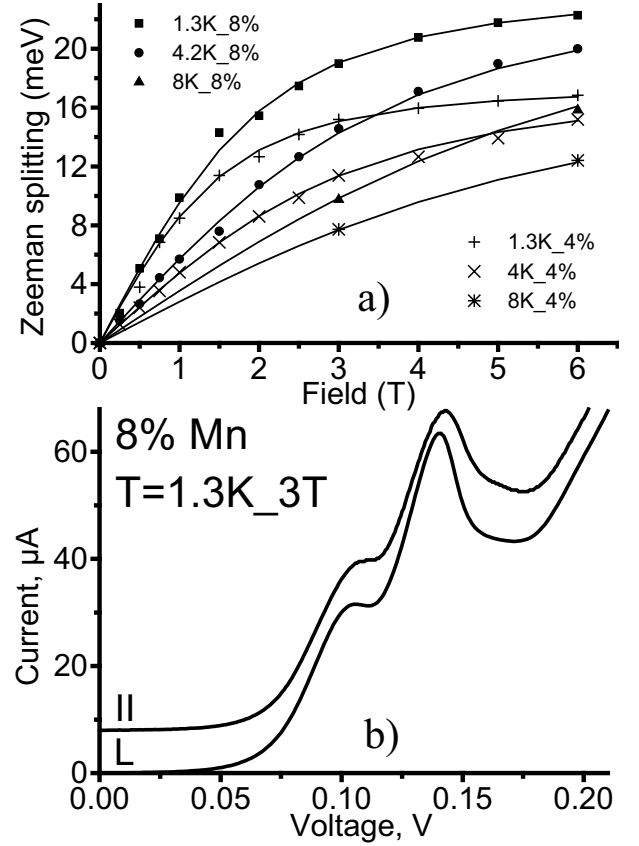


FIG. 3: a) Giant Zeeman splitting versus magnetic field for both samples. The lines come from a Brillouin like description of the well levels. The symbols represent the splitting in the peak positions extracted from the experimental data. b) I-V curves for sample with 8% Mn, under 3T in plane (II) or perpendicular (L) magnetic field.

well, which are at higher energy than the zero momentum ground state. Furthermore, the spread in in-plane k vectors leads to a broadening of the tunnelling resonance [17, 18]. From the figure, it is obvious that the splitting of the resonance peak is similar in both orientations of magnetic field. This is due to the isotropic g-factor in the DMS. This observation directly rules out any explanation of the peak structure as resulting from Landau level splitting in the quantum well.

Temperature dependent measurements of the 6T I-V curves are presented in Fig. 4, again with the curves offset for clarity. Qualitatively, an increase in temperature has a similar effect on the I-V curves as a reduction of the magnetic field (cf. Equ. 1). The peaks move closer together and eventually merge back into a single peak. On the other hand, the zero field I-V curves are practically temperature independent in the range from 1.3 Kelvin to 30 Kelvin. The reduction of the splitting as a function of field can be anticipated from the results of Fig. 3, and is simply a manifestation of the temperature dependence of the giant Zeeman splitting of the DMS. This suggests that any operational limit imposed on the device by tem-

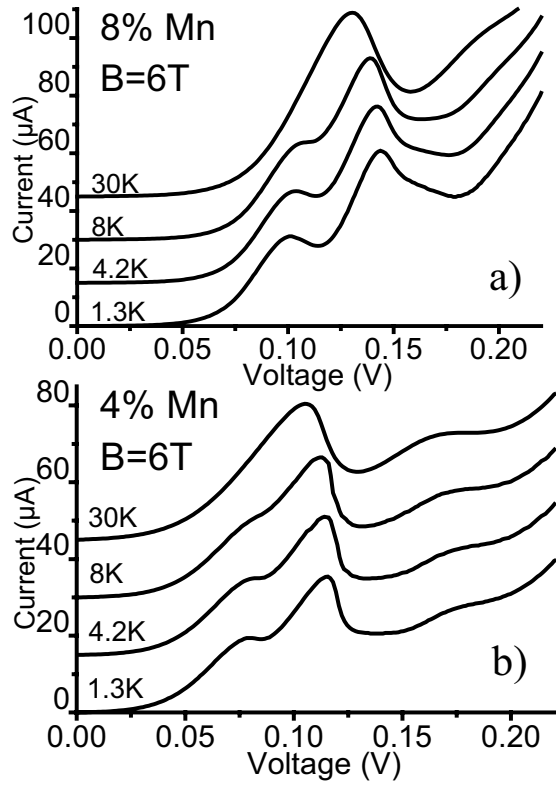


FIG. 4: Temperature dependence of the I-V curves of the first resonance, shown for each of the diodes.

perature is purely a function of the material in the well, and that no inherent limit from the tunnelling process is detected.

In summary, we have presented results of all II-VI semiconductor RTDs based on the (Zn,Be)Se system, with magnetic impurities (Mn) in the quantum well. A strong splitting of quantum well resonance is observed as a function of magnetic field, which originates from the Giant Zeeman splitting of the spin levels in the dilute magnetic semiconductor quantum well. An intuitive model that simulates the magnetic field dependence of the I-V characteristic of the device is discussed, and shows good agreement with the experiment. The results therefore demonstrate the possibility of devices based on tunnelling through spin resolved energy levels. Experiments aiming to measure the spin polarisation of the current flowing through such a device are currently underway.

Acknowledgments

The authors would like to thank G. Austing, H. Buhmann, L. Eaves, A. Gröger and J. Wang for useful discussions and V. Hock for sample fabrication, as well as DFG (SFB 410), BMBF, the DARPA Spins program and ONR for financial support.

-
- [1] G. Schmidt, D. Ferrand, L.W. Molenkamp, A.T. Filip, B.J. van Wees, Phys. Rev. B 62, 4790 (2000).
 - [2] E.I. Rashba, Phys. Rev. B 62, 16267, (2000).
 - [3] A. Fert and H. Jaffrès, Phys. Rev. B 64, 184420, (2001).
 - [4] R. Fiederling, M. Keim, G. Reuscher, W. Ossau, G. Schmidt, A. Waag, and L.W. Molenkamp, Nature 402, 787 (1999).
 - [5] Y. Ohno, D.K. Young, B. Beschoten, F. Matsukura, H. Ohno, D.D. Awschalom, Nature 402, 790 (1999).
 - [6] G. Schmidt, G. Richter, P. Grabs, C. Gould, D. Ferrand, L.W. Molenkamp, Phys. Rev. Lett. 87, 227203 (2001).
 - [7] V.F. Motsnyi, J. de Boeck, J. Das, W. Van Roy, G. Borghs, E. Goovaerts, V.I. Safarov, Appl. Phys. Lett. 81, 265 (2002).
 - [8] D.P. DiVincenzo, JAP 85, 4785 (1999).
 - [9] Th. Gruber, M. Keim, R. Fiederling, G. Reuscher, W. Ossau, G. Schmidt, L.W. Molenkamp, and A. Waag, Appl. Phys. Lett. 78, 1101, (2001).
 - [10] M.L. Leadbeater, E.S. Alves, L. Eaves, M. Henini, O.H. Hughes, A. Celesta, J.C Portal, G. Hill, and M.A. Pate, Phys. Rev. B, 39, 3438, (1989).
 - [11] A.D. Martin, M.L.F. Lerch, P.E. Simmonds and L. Eaves, Appl. Phys. Lett. 64, 1248 (1994).
 - [12] M. L. F. Lerch, A. D. Martin, P. E. Simmonds, L. Eaves, and M. L. Leadbeater, Solid-St. Electron. 37, 961 (1994)
 - [13] J. A. Gaj, R. Planel, G. Fishman, Solid State Commun. 29, 435 (1979).
 - [14] W. Y. Yu, A. Twardowski, L. P. Fu, A. Petrou, B. T. Jonker, Phys. Rev. B51, 9722 (1995).
 - [15] A. Twardowski, M. von Ortenberg, M. Demianiuk, R. Pauthenet, Solid State Commun. 51, 849 (1984).
 - [16] *Landolt-Börnstein, New Series III/22a*, edited by O. Madelung (Springer-Verlag, Berlin 1987), p. 181.
 - [17] S. Ben Amor, K.P. Martin, J.J.L. Rascol, R.J. Higgins, A. Torabi, H.M. Harris, and C.J. Summers, Appl. Phys. Lett. 53, 2540, (1988).
 - [18] R.A. Davies, D.J. Newson, T.G. Powell, M.J. Kelly and H.W. Myron, Semicon. Sci. Technol. 2, 61, (1987).